Proton–proton total cross-sections at VHE from accelerator data

J Pérez-Peraza[1,4], **A Sánchez-Hertz**[1], **M Alvarez-Madrigal**[1], **A Gallegos-Cruz**[2], **J Velasco**[3,4] **and A Faus-Golfe**[3]

[1] Instituto de Geofísica, UNAM, Ciudad Universitaria, Coyoacán 04510, México DF, Mexico
[2] Ciencias Básicas, UPIICSA, IPN, Iztacalco 08400, Mexico DF, Mexico
[3] IFC—Instituto de Física Corpuscular, Centro Mixto CSIC–Universitat de València, Burjassot 46100, Valencia, Spain
E-mail: perperaz@igeofcu.unam.mx and velasco@ific.uv.es

Abstract. Up-to-date estimates of proton–proton total cross-sections, σ_{tot}^{pp}, at very high energies in the literature were obtained from cosmic rays ($> 10^{17}$ eV) by approximations using the measured proton–air cross-section at these energies. As σ_{tot}^{pp} are measured with present day high energy colliders up to nearly 2 TeV in the centre of mass ($\sim 10^{15}$ eV in the laboratory), several proven theoretical, empirical and semi-empirical parametrizations for interpolation at accelerator energies were used to extrapolate these measured values to get reasonable estimates of cross-sections at higher cosmic ray energies ($\sim 10^{17}$ eV). The cross-section estimates from these two methods disagree by a discrepancy beyond statistical error. Here we use a phenomenological model based on the 'multiple diffraction' approach to successfully describe data at accelerator energies. Using this model, we then estimate σ_{tot}^{pp} at cosmic ray energies. The model free-parameters used in the fit depend on only two physical observables: the differential cross-section and the parameter ρ. The model estimates of σ_{tot}^{pp} are then compared with total cross-section data. Using regression analysis, we determine confidence error bands, analysing the sensitivity of our predictions to the data used in the extrapolations. This work reduces the width of the confidence band around 'multiple diffraction' model fits of accelerator data. With the data at 546 GeV and 1.8 TeV, our extrapolations are compatible with only the Akeno cosmic ray data, predicting

[4] Author to whom any correspondence should be addressed.

a slower rise with energy than do other cosmic ray results and other extrapolation methods. We discuss our results within the context of constraints expected from future accelerator and cosmic ray experimental results.

Contents

1. Introduction

Recently a number of difficulties in uniting accelerator and cosmic ray values of the hadronic total cross-sections for proton–proton (p–p), σ_{tot}^{pp}, and antiproton–proton, $\sigma_{tot}^{\bar{p}p}$, in the light of the best recent data have been summarized [1]. A united picture would be of the highest importance for the interpretation of results of new cosmic ray experiments such as the HiRes [2] and in designing proposals that are currently in progress as the Auger Observatory [3], as well as in designing detectors for future accelerators, such as the CERN pp Large Hadron Collider (LHC) [4]. Although most accelerator measurements of σ_{tot}^{pp} and $\sigma_{tot}^{\bar{p}p}$ at centre of mass energies $\sqrt{s} \leqslant 1.8\,\text{TeV}$ are fairly consistent (see figure 1 where the 1.8 values just embrace the 85% bands), unfortunately above $\sqrt{s} > 6\,\text{TeV}$ cosmic ray experiments agree among themselves only because of their large uncertainty bands (section 3); 7.5–23% for three experiments at 30 TeV and (3–19)% for 2 experiments at 40 TeV. It is more disturbing that they are consistent with different predictions from the extrapolation of accelerator data up to cosmic ray energies, again only because of their own uncertainty and that of the extrapolations. Some extrapolations predict smaller values of σ_{tot}^{pp} than those of cosmic ray experiments (e.g. [5, 6]); others agree at some specific energies with cosmic ray results (e.g. [7]). Dispersion of cosmic ray results is associated mainly with the strong model-dependence of the relationship of the basic hadron–hadron cross-section and the hadronic cross-section in air. The latter determines the attenuation length of hadrons in the atmosphere, which is usually measured in different ways, and depends strongly on the rate (k) of energy dissipation of the primary proton into the electromagnetic shower observed by the experiment. Such a cascade is simulated by different Monte Carlo techniques

implying additional discrepancies between different experiments. Furthermore, σ_{tot}^{pp} in cosmic ray experiments is determined from σ_{p-air}^{inel} using a nucleon–nucleon scattering amplitude which is frequently in disagreement with most accelerator data [1].

Although in principle QCD theory gives the exact description of strong interactions, its practical application in the study of hadronic interactions is still limited. In the absence of a pure QCD description, phenomenological models are used to compare experimental data with theoretical schemas. These models are based on general principles, such as 'unitarity', 'analycity' and 'cross-symmetry' and have proven to be successful in the comprehension and prediction of the hadronic amplitude behaviour at high energies [8]. Consequently, a wide range of possibilities is open for the development of models of this kind. Several classifications of phenomenological models have been made according to the general principles on which they are based (e.g. [9]), geometrical scaling models [10], diffraction-dominance models [11], factorized eikonal type models [12] and Reggeon-field-theory models [13]. At present, the more frequently used models (e.g. [14]) are (a) 'analytic amplitude' models based on solutions of the derivative dispersion relations; (b) 'eikonal' models. In the context of (a) outstanding work has been done by several authors (e.g. [6], [15]–[21]), however, the most complete and systematic work, to our knowledge, has been developed in association with the COMPETE Collaboration, in accord with the Regge–Pomeranchuk–Heisenberg type parametrizations and the 'general principles' previously mentioned [22]–[28]. Such systematization has been carried out on the selection and the cleaning of data as well as the application of models and fitting techniques, refining the conventional way (χ^2) of measuring the goodness-of-fits, by means of seven statistical indicators related to the data and to the process used to obtain them [25]. The results of this series of work have been of great relevance in the context of hadronic interactions. The present work falls within the framework of models of the type (b) in the impact parameter representation, using 'multiple diffraction' theory [29] to first-order and parametrization of the hadronic form factors and the elemental dispersion amplitude contained in the eikonal. We use an alternative statistical technique to evaluate error bars in the extrapolation process, called the 'forecasting' method. This work produces an improved accelerator extrapolation which both lowers the predicted p–p total cross-section curve and narrows its confidence bands, making it less consistent with most cosmic rays showers [9] and most of the [30] results as feared.

Thus, we dispose of many parametrization models (purely theoretical, empirical or semi-empirical based) that fit the accelerator data fairly well. Most of them agree that at the energy of the future LHC (14 TeV in the centre of mass) or higher, the rise with energy of σ_{tot}^{pp} will continue, although the predicted values differ from model to model. Both the cosmic ray and accelerator approaches should complement each other in order to draw the best description of the p–p hadronic cross-section behaviour at ultra high energies. However, the present status is that since the interpolation of accelerator data is nicely obtained with most parametrization models, it has been hoped that their extrapolation to higher energies might yield high confidence values. The accelerator parametrizations are usually based on a small number of fundamental parameters, in contrast to the difficulties found in deriving σ_{tot}^{pp} from cosmic ray results [1]. With the aim of elucidating the problem, we first briefly analyse the way estimates are made for σ_{tot}^{pp} from accelerators in section 2 and from cosmic rays in section 3. We find serious discrepancies in both estimation methodologies. In section 4 we describe the 'multiple diffraction' model and the method used to evaluate the model parameters on the basis of only two data-based physical observables: the differential cross-section and the parameter ρ. For the goal of the present study, we neglect crossing symmetry. In section 5, we present a suitable parametrization to high energies

of the free energy-dependent parameters of the model, and we discuss its physical significance. In section 6 we describe the procedure for the determination of error bands as per appendix A. In section 7, on the basis of the 'multiple diffraction' model applied to accelerator data, we predict σ_{tot}^{pp} values with high confidence levels (CL). In section 8, we discuss our results in terms of the hypothesis $\sigma_{tot}^{\bar{p}p} = \sigma_{tot}^{pp}$, and finally in section 9, we conclude with a discussion of the implications of extrapolations within the framework of present cosmic ray estimates.

2. Hadronic σ_{tot}^{pp} from accelerators

Ever since the first results of the Intersecting Storage Rings (ISR) at CERN arrived in the 1970s, it is well established that σ_{tot}^{pp} rises with energy [31, 32]. The CERN $S\bar{p}pS$ collider found this rise valid for $\sigma_{tot}^{\bar{p}p}$ as well [33]. Later, the Tevatron at Fermilab confirmed that for $\sigma_{tot}^{\bar{p}p}$ the rise continues at 1.8 TeV, even if different experiments disagree as to the exact value [34]–[36]. A full discussion of these problems may be found in [37, 38]. The amount of the rise of the total cross-section at those energies is still to be determined. Let us resume the standard technique used by accelerator experimentalists [6].

Using a semi-empirical parametrization based on Regge theory and asymptotic theorems, experimentalists have successively described their data from the ISR to the $S\bar{p}pS$ energies. It takes into account all the available data for σ_{tot}^{pp}, ρ^{pp}, $\sigma_{tot}^{\bar{p}p}$ and $\rho^{\bar{p}p}$, where $\rho^{pp,\bar{p}p}$, is the ratio of the real to the imaginary part of the (pp, $\bar{p}p$) forward elastic amplitude at time zero. The fits are performed using the once-subtracted dispersion relations:

$$\rho_\pm(E)\sigma_\pm(E) = \frac{C_s}{p} + \frac{E}{\pi p} \int_m^\infty dE' p' \left\{ \frac{\sigma_\pm(E')}{E'(E'-E)} - \frac{\sigma_\mp(E')}{E'(E'+E)} \right\}, \tag{1}$$

where C_s is the subtraction constant. The expression for $\sigma_{tot}^{pp,\bar{p}p}$ is

$$\sigma_{-,+}^{tot} = A_1 E^{-N_1} \pm A_2 E^{-N_2} + C_0 + C_2 \left[\ln\left(\frac{s}{s_0}\right) \right]^2, \tag{2}$$

where $-$, $+$ stands for pp ($\bar{p}p$) scattering. Cross-sections are measured in mb and energy in GeV, E being the energy measured in the laboratory frame. The scale factor s_0 has been arbitrarily chosen to equal $1\,\text{GeV}^2$. The most interesting term is the one controlling the high-energy behaviour, given by a $\ln^2(s)$ factor, being compatible, asymptotically, with the Froissart–Martin bound [39]. The parametrization assumes σ_{tot}^{pp} and $\sigma_{tot}^{\bar{p}p}$ to be the same asymptotically. This is justified by the very precise measurement of the $\rho_{\bar{p}p}$ parameter at 546 GeV at the $S\bar{p}pS$ collider, $\rho_{\bar{p}p} = 0.135 \pm 0.015$ [40], which implies that at present there is no sizeable contribution of the odd under crossing part of the forward amplitude, the so-called 'Odderon hypothesis'. This hypothesis predicts a value of $\rho_{\bar{p}p} > 0.17$–0.20 [41, 42], that is, greater than the $S\bar{p}pS$ value. The eight free parameters are determined by a fit which minimizes the X^2 function:

$$X^2 = X_{\sigma_{\bar{p}p}}^2 + X_{\rho_{\bar{p}p}}^2 + X_{\sigma_{pp}}^2 + X_{\rho_{pp}}^2. \tag{3}$$

The fit has proved its validity predicting from the ISR pp and $\bar{p}p$ data (ranging from 23 to 63 GeV in the centre of mass), the $\sigma_{tot}^{\bar{p}p}$ value [15] later found at the $S\bar{p}pS$ collider, one order of magnitude higher in energy (546 GeV) [33]. With the same well-known method and using the most recent results, it is possible to get estimates for σ_{tot}^{pp} at the LHC and higher energies. These estimates, together with our present experimental knowledge of both σ_{tot}^{pp} and $\sigma_{tot}^{\bar{p}p}$ are plotted in
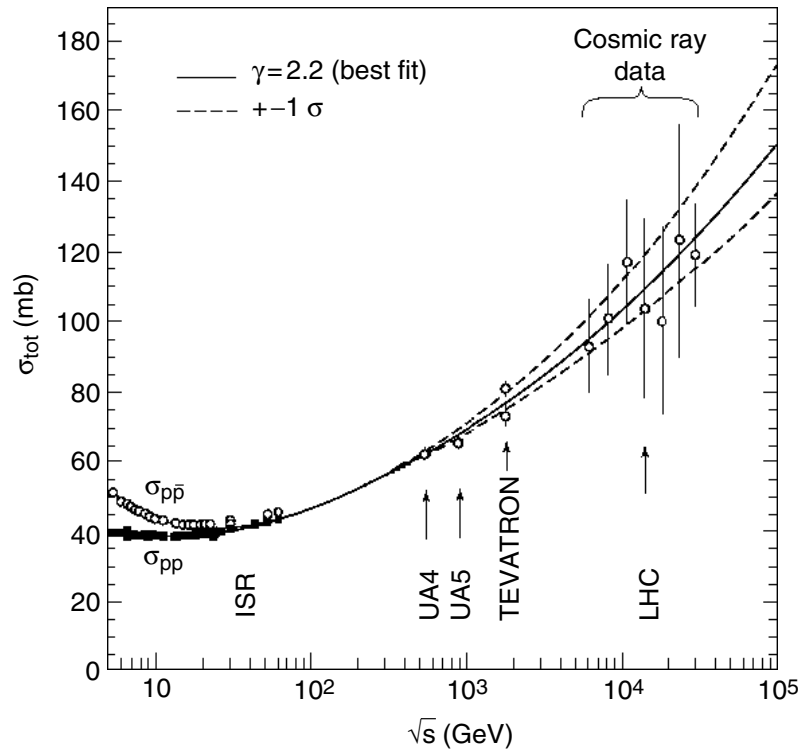
Figure 1. σ_{exp}^{tot} from accelerator and from cosmic rays: the solid line indicates the best χ^2 fit obtained from a semi-empirical parametrization [6]. The two dashed lines delimit the region of uncertainty. Cosmic ray estimations from [43].

Table 1. $\sigma_{tot}^{\bar{p}p}$ data from high energy accelerators: fit values are from [6].

$\sqrt{s}$ (TeV)	σ_{tot}^{pp} (mb)
0.55	
Fit	61.8 ± 0.7
UA4	62.2 ± 1.5
CDF	61.5 ± 1.0
1.8	
Fit	76.5 ± 2.3
E710	72.8 ± 3.1
CDF	80.3 ± 2.3
E811	71.7 ± 2.0
16.0	
Fit	111.0 ± 8.0
40.0	
Fit	130.0 ± 13.0

figure 1. We have also plotted the cosmic ray experimental data from AKENO (now AGASSA) [43] and the Fly's Eye experiment [44, 45]. The curve is the result of the fit described in [6]. The increase in σ_{tot}^{pp} as the energy increases is clearly seen.

Numerical predictions from this analysis are given in table 1. It should be remarked that at the LHC energies and beyond, the predicted σ_{tot}^{pp} and $\sigma_{tot}^{\bar{p}p}$ values from the fit display relatively

high error values ($\Delta\sigma^{tot}_{pred} \geqslant 8\,\text{mb}$). Also, recent analysis using both cosmic ray and accelerator data calculated relatively wide extrapolated error bands, for example 5–7 mb at 14 TeV [46]. It follows that ways to reduce the uncertainties and hence improve extrapolations are needed.

3. Hadronic σ^{pp}_{tot} from cosmic rays

Cosmic ray experiments give us σ^{pp}_{tot} indirectly from extensive cosmic ray air shower (EAS) data. As summarized in [1] and widely discussed in the literature, the determination of σ^{pp}_{tot} is a rather complicated process with at least two well-differentiated steps. In the first place, the primary interaction involved in and determined through EAS is proton–air, yielding the p-inelastic cross-section, σ^{p-air}_{inel}, using some measure of the attenuation of the rate of showers deep in the atmosphere, Λ_m:

$$\Lambda_m = k\lambda_{p-air} = k\frac{14.5m_p}{\sigma^{p-air}_{inel}}. \tag{4}$$

The k factor parametrizes the rate at which the energy of the primary proton is dissipated into electromagnetic energy. A simulation with a full representation of the hadronic interactions in the cascade is needed to calculate it. This is done by means of Monte Carlo simulations [47]–[49].

Secondly, the connection between σ^{p-air}_{inel} and σ^{pp}_{tot} is model dependent. A theory for nuclei interactions must be used, which is usually Glauber's theory [29, 50]. The whole procedure makes it difficult to get a general accepted value for σ^{pp}_{tot}. Depending on the particular assumptions made, the values may range by large amounts, from as low as 122 ± 11 at $\sqrt{s} = 30$ TeV quoted by the Fly's Eye group [44, 45] to 133 ± 10 mb by the 'Akeno Collaboration' [43], also at $\sqrt{s} = 30$, to 162 ± 38 mb at nearly $\sqrt{s} = 30$ (around 160–170 mb $\sqrt{s} = 40$ TeV) [30] and even as high as 175^{+40}_{-27} at $\sqrt{s} = 40$ TeV [9]. It should be realized that the three values at 30 TeV do overlap within their errors as do the two values at 40 TeV. In the 40 TeV cases, even taking into account the large quoted errors, the values for σ^{pp}_{tot} are hardly compatible with the values obtained from the extrapolations of current accelerator data.

These results do not offer cosmic ray estimations of σ^{pp}_{tot} much help in constraining extrapolations from accelerator energies. Conversely we could ask if a reliable extrapolation based on accelerator data could be used to constrain cosmic ray interpretations.

4. A 'multiple diffraction' approach for evaluation of σ^{pp}_{tot}

Let us tackle the mismatch of accelerator and cosmic ray estimates using the multiple diffraction model applied to hadron–hadron scattering [51]. The elastic hadronic scattering amplitude for the collision of two hadrons A and B, neglecting spin, is described as

$$F(q, s) = \mathrm{i} \int_0^\infty b\,\mathrm{d}b[1 - \mathrm{e}^{\mathrm{i}\xi(b,s)}]J_o(qb), \tag{5}$$

where $\xi(b, s)$ is the eikonal, b the impact parameter, J_o the zero-order Bessel function and $q^2 = -t$ the four-momentum transfer squared. In the first 'multiple diffraction' theory, the eikonal in the transferred momentum space is proportional to the product of the hadronic form factors G_A

and G_B (geometry) and the averaged elementary scattering amplitude among the constituent partons f (dynamics), and can be expressed to first order as $\xi(b, s) = C_{A,B}\langle G_A G_B f\rangle$, where the proportionality factor $C_{A,B}$ is the free parameter known as the 'absorption factor', and the brackets denote the symmetrical two-dimensional Fourier transform. A connection between theory and experiment may be obtained by means of hadronic factors and elementary parton–parton amplitudes, which are not physical observables. However with the help of the optical theorem σ_{tot}^{pp} may be evaluated in terms of the elastic amplitude $F(q, s)$:

$$\sigma_{tot}^{pp} = 4\pi \operatorname{Im} F(q = 0, s), \tag{6}$$

σ_{tot}^{pp} is a physical observable. The other two physical observables are the differential elastic cross-section and ρ expressed respectively as

$$\frac{\mathrm{d}\sigma}{\mathrm{d}q^2} = \pi |F(q, s)|^2 \tag{7}$$

and

$$\rho = \frac{\operatorname{Re} F(q = 0, s)}{\operatorname{Im} F(q = 0, s)}. \tag{8}$$

'Multiple diffraction' models differ from one another by the particular choice of parametrizations made for G_A and G_B and the elementary amplitude f. Hereafter we will adopt the model proposed in [7], which has the advantage of using a small set of five free parameters which are in principle energy dependent. Two of them (α^2, β^2) are associated with the form factor

$$G = \left(1 + \frac{q^2}{\alpha^2}\right)^{-1} \left(1 + \frac{q^2}{\beta^2}\right)^{-1}. \tag{9}$$

The other three (C, a, λ) are associated with the elementary complex amplitude f

$$f(q, s) = \operatorname{Re} f(q, s) + \mathrm{i} \operatorname{Im} f(q, s), \tag{10}$$

where

$$\operatorname{Im} f(q, s) = C\frac{1 - \frac{q^2}{a^2}}{1 - \frac{q^4}{a^4}} \tag{11}$$

and

$$\operatorname{Re} f(q, s) = \lambda(s)\operatorname{Im} f(q, s), \tag{12}$$

so that

$$\operatorname{Im} F(q = 0, s) = \int_0^\infty [1 - \mathrm{e}^{-\Omega(b,s)} \cos\{\lambda\Omega(b, s)\}] \, b \, \mathrm{d}b \, J_o(q, b)|_{q=0}, \tag{13}$$

with the opacity $\Omega(b, s)$ given as

$$\Omega(b, s) = \int_o^\infty G^2 \operatorname{Im} f(q, s) \, J_o(q, b) \, q \, \mathrm{d}q \tag{14}$$

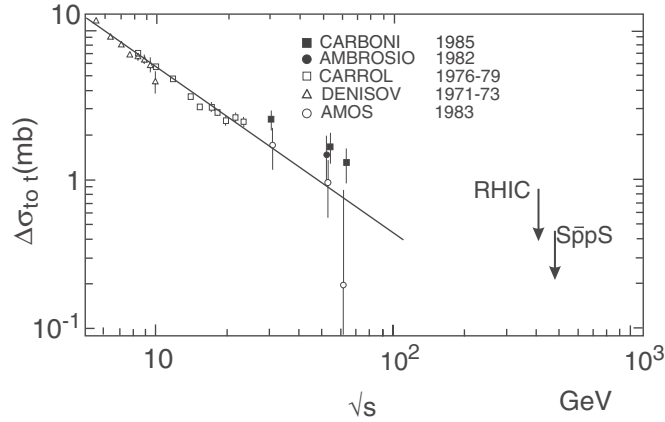Institute *of* **Physics** Φ DEUTSCHE PHYSIKALISCHE GESELLSCHAFT

Figure 2. Plot of $\Delta\sigma_{tot} \equiv \sigma^{tot}_{\bar{p}p} - \sigma^{tot}_{pp} \sim s^{-0.56}$ indicating that $\Delta\sigma^{tot}$ tends towards zero up to centre-of-mass energies ~ 60 GeV. Data points are from [55].

whose explicit expression is

$$\Omega(b, s) = C\{E_1 K_0(\alpha b) + E_2 K_0(\beta b) + E_3 K_{ei}(ab) + E_4 K_{er}(ab) \\ + b\,[E_5 K_1(\alpha b) + E_6 K_1(\beta b)]\}, \tag{15}$$

where k_0, k_1, k_{ei}, and k_{er} are the modified Bessel functions, and E_1–E_6 are functions of the five free parameters. The p–p total cross-section is directly determined by the expression

$$\sigma^{pp}_{tot} = 4\pi \int_o^\infty b\,\mathrm{d}b\{1 - \mathrm{e}^{-\Omega(b,s)}\cos[\lambda\Omega(b,s)]\}J_o(q, b)|_{q=0}, \tag{16}$$

which was numerically solved in [52, 53]. It should be noted that, according to the principle of 'analyticity', the scattering forward amplitude for particle–particle and particle–antiparticle both come from the same analytical function [8]. The total cross-sections of both reactions are assumed to behave in one of the following ways: up to the ISR energies the differences are attributed to Regge contributions, which are expected to disappear at higher energies [5, 54], or the differences are interpreted in terms of the 'maximal Odderon hypothesis', which predicts that they increase as the energy passes the highest energy of the ISR. At this point, the following understanding must be emphasized as essential in the rest of this study. Firstly, we quote the success in the prediction of $\sigma^{\bar{p}p}_{tot}$ at the $S\bar{p}pS$ collider [33] from the ISR data (mainly pp) using expressions (1) and (2), where σ^{pp}_{tot} and $\sigma^{\bar{p}p}_{tot}$ were taken to be asymptotically equal [15]. Secondly, according to [55] the difference $\Delta\sigma = \sigma^{\bar{p}p}_{tot} - \sigma^{pp}_{tot}$, tends toward zero as $s^{-0.56}$ up to energies $\leqslant 2000$ GeV in the laboratory (~ 60 GeV in the centre of mass; figure 2). And thirdly, we are aware that it can be argued that σ^{pp}_{tot} and $\sigma^{\bar{p}p}_{tot}$ are different for higher energies, but as indicated in section 2 current evidence indicates the contrary.

In the face of this triple line of evidence, in our 'multiple diffraction' analysis, the same behaviour for both σ^{pp}_{tot} and $\sigma^{\bar{p}p}_{tot}$ at high energy is assumed. So, here after $\sigma^{pp}_{tot} = \sigma^{\bar{p}p}_{tot} = \sigma_{tot}$. It is noteworthy that some parametrization models, as RRP [56], predict the same value for both cross-sections at $\sqrt{s} > 70$ GeV and the same value for the corresponding ρ at $\sqrt{s} > 110$ GeV.
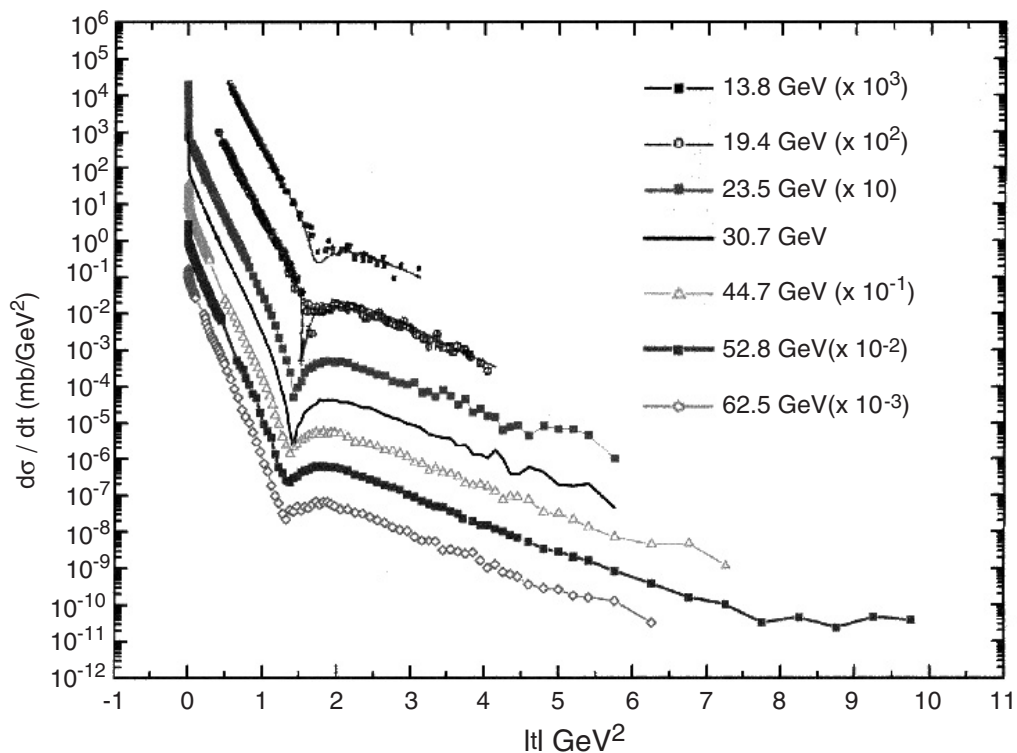
Figure 3. Data of *pp* differential cross-section at $\sqrt{s} \leqslant 62.5$ according to [58]–[62].

4.1. Evaluation of the model parameters

For the evaluation of the free parameters it was assumed, following [7] that two of them are constants: $a^2 = 8.2\,\text{GeV}^2$ and $\beta^2 = 1.8\,\text{GeV}^2$. The other three parameters are: $C(s)$ and $\alpha^{-2}(s)$ which determine the imaginary part of the hadronic amplitude (equation (11)) and consequently the total cross-section (equation (6)), as well as $\lambda(s)$ which controls the real part of the amplitude (equation (12)). Setting $\lambda(s) = 0$ makes the amplitude purely imaginary, so that a zero (a minimum) is produced in the dip region, where only the real part of the amplitude becomes important [57]. We fit experimental data (figure 3) of the elastic differential cross-section, $\mathrm{d}\sigma/\mathrm{d}q^2$, with equation (7), choosing the set (C, α^{-2}) for which the theoretical and the experimental central values are equated at the precise $t\ (\text{GeV}/c)^2$ value where the data show its first minimum (the 'dip' position), which coincides with the minimum of the imaginary part of the elastic amplitude. Throughout we use units where $c = 1$. Data of *pp* differential cross-section at 13.8 and 19.4 GeV were taken from [58], for 23.5–62.5 GeV from [59], for 546 GeV ($\bar{p}p$) from [60], with ($-t < 0.5\,\text{GeV}^2$) and from [61] with ($0.5 \leqslant -t \leqslant 1.55\,\text{GeV}^2$), and for 1800 GeV from [62] with ($0.034 \leqslant -t \leqslant 0.65\,\text{GeV}^2$). The procedure is carried out at each energy where there are available accelerator data for $\mathrm{d}\sigma/\mathrm{d}q^2$ in the interval $13.8 \leqslant \sqrt{s} \leqslant 1800\,\text{GeV}$, as illustrated in figures 4 and 5. Because data error bars at the dip position are small the fitting procedure is based on the central values. It must be emphasized that, it is precisely because the minimum of the imaginary amplitude is produced in the dip region, that data at 1800 eV are quite suitable for our procedure, since the predicted minimum falls at $t = 0.585\,\text{GeV}^2$ where data are available
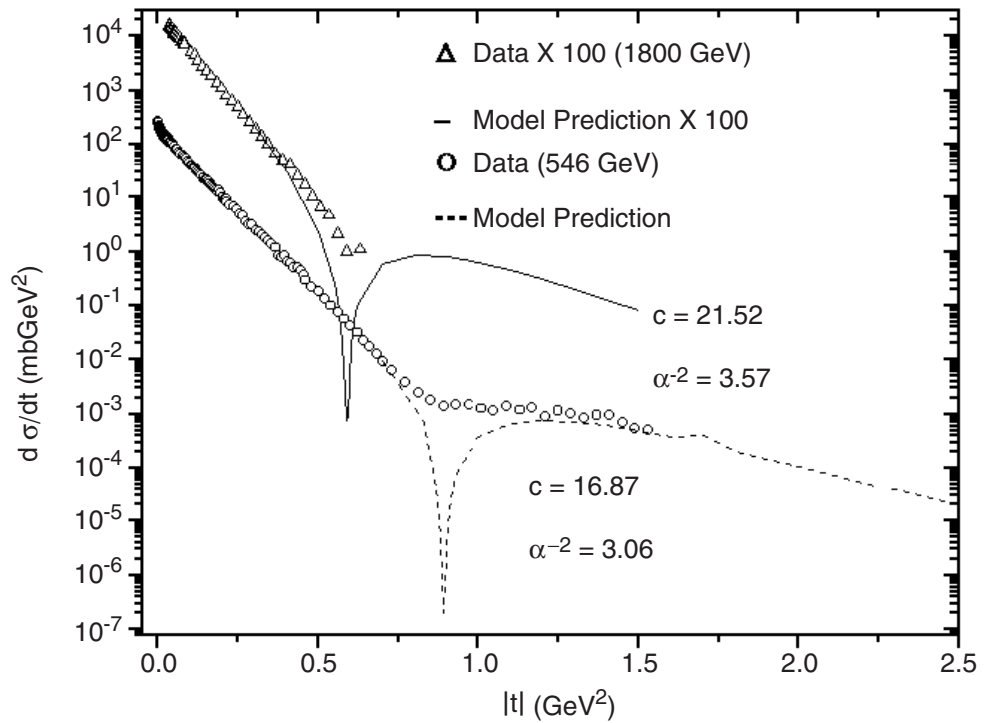
Figure 4. Fits of the predicted imaginary amplitude to data of the $\bar{p}p$ differential cross-sections to determine $C(s)$ and $\alpha^{-2}(s)$ by equating experimental and theoretical values at the specific $|t|$ of the 'dip' position for $\sqrt{s} = 546\,\text{GeV}$ and $\sqrt{s} = 1800\,\text{GeV}$.
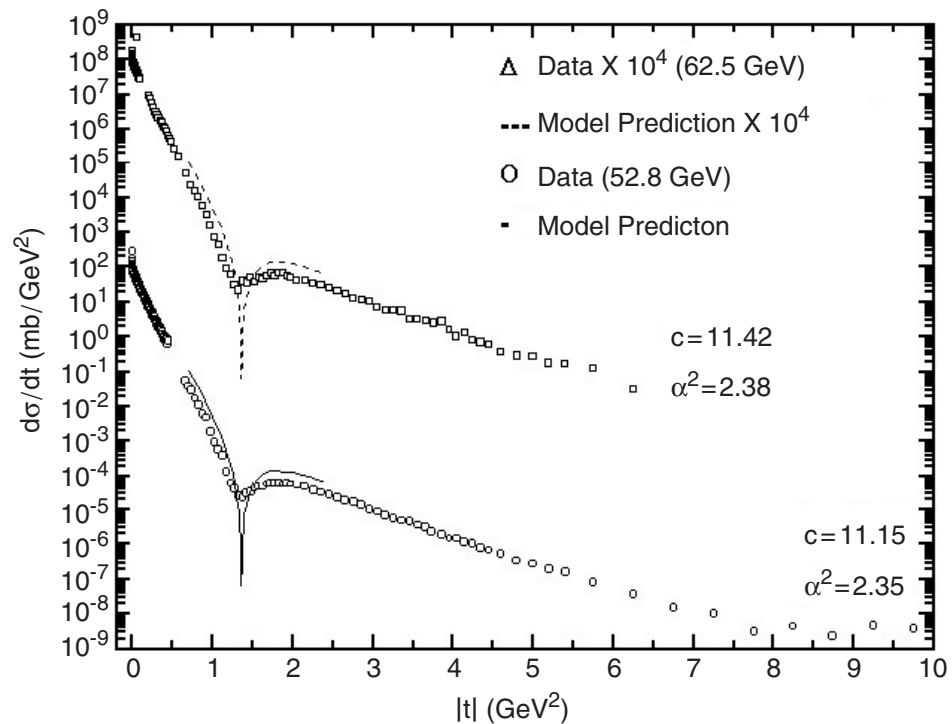

Figure 5. Same as figure 4 but for $\sqrt{s} = 52.8$ and $62.5\,\text{GeV}$.

Table 2. Values of the parameters C, α^{-2} and λ at each energy. They are obtained by equating the accelerator data and the model prediction for the elastic differential cross-sections and for the parameter ρ in the interval $13 \leqslant \sqrt{s} \leqslant 62.5$ and $546 \leqslant \sqrt{s} \leqslant 1800\,\text{GeV}$.

$\sqrt{s}$ (GeV)	$C(s)$ (GeV^{-2})	$\alpha^{-2}(s)$ (GeV^{-2})	$\lambda(s)$
13.8	9.97	2.092	-0.126
19.4	10.05	2.128	-0.043
23.5	10.25	2.174	0.025
30.7	10.37	2.222	0.053
44.7	10.89	2.299	0.079
52.8	11.15	2.350	0.099
62.5	11.42	2.380	0.115
546	16.90	3.060	0.182
1800	21.52	3.570	0.194

($\text{d}\sigma/\text{d}t = 0.0101$). The next datum at $t = 0.627\,\text{GeV}^2$ shows a slight increase. Furthermore, the shift of the dip region towards lower values of t as energy increases is qualitatively consistent with the expectation relative to the shoulder at $546\,\text{GeV}$ ($t = 0.9\,\text{GeV}^2$). Once the values of $C(s)$ and $\alpha^{-2}(s)$ are determined for each energy they are introduced along with the constant parameters a^2 and β^2 into equation (8).

We determine values for $\lambda(s)$ which produce the experimental value of $\rho(s)$, for each energy, $\sqrt{s}$, where there are available accelerator data in the interval $13.8 \leqslant \sqrt{s} \leqslant 1800\,\text{GeV}$. The central values of the three energy-dependent free parameters, $C(s)$, $\alpha^{-2}(s)$ and $\lambda(s)$ obtained are listed in table 2. Therefore, the method employed to evaluate the model parameters only requires $\text{d}\sigma/\text{d}t$ and $\rho(s)$ data.

5. Parametrization for extrapolation to high energies

Despite other successes of the theory, the microscopic basis, in terms of QCD, of the physics behind the parametrization and fitting procedures have not been completely developed because the hadron diffractive phenomenon in question is essentially a non-perturbative problem with which confinement is still unsolved. However, the closeness of our fits to the collider data (ISR, $S\bar{p}pS$ and Tevatron) suggest that the basic approach of the limited model used here is correct, as described for instance in [51]. Indeed, even with the approximation made in ignoring crossing symmetry, the parametrization process followed here could not be arbitrary. That said, for interpolations and extrapolations, we made parametrizations of the three energy-dependent free parameters. Using the values obtained for those parameters, as described in table 2 and following the procedure to be described in section 6, a second-order fit of the values of $C(s)$ and $\alpha^{-2}(s)$ and a exponential fit of $\lambda(s)$ have been obtained from the following analytical expressions:

$$C(s) = 19.24521 - 2.86114 \ln s + 0.22616 \ln s^2, \tag{17}$$

$$\alpha^{-2}(s) = 1.8956 - 0.03937 \ln s + 0.01301 \ln s^2, \tag{18}$$

$$\lambda(s) = 0.01686 + 0.00125 \left(1 - \mathrm{e}^{-\ln(s/400)/0.18549} \right) + 0.19775 \left(1 - \mathrm{e}^{-\ln(s/400)/3.74642} \right). \tag{19}$$
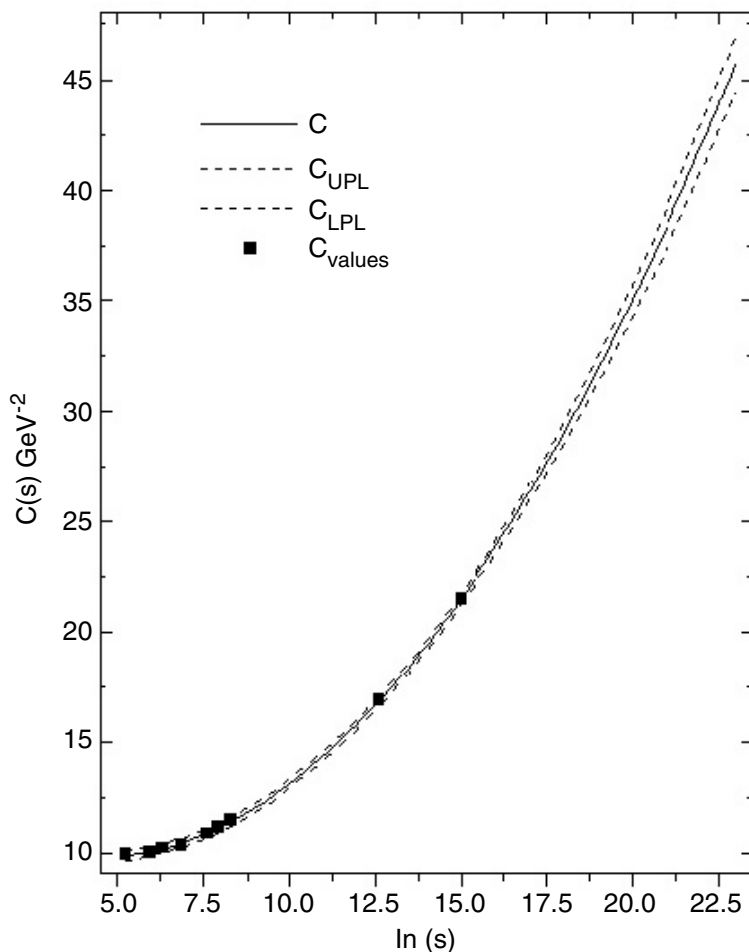
Figure 6. The parameter $C(s)$ from table 2 with its confidence interval.

Results are displayed in table 2 and illustrated in figures 6–8 as the central-solid lines. However, the reliability of the functional parametrizations for extrapolations must have physical support, since it is clear that several parametrizations that may correctly describe the data in the range $13.8 \leqslant \sqrt{s} \leqslant 1800\,\text{GeV}$, may not remain consistent but differ substantially when extrapolated to high energies. Thus parametrization selections should be restricted according to the physical information available. As mentioned before, the fits of $C(s)$ and $\alpha^{-2}(s)$ in the limited experimental range were based on experimental data of the differential cross-section and $\rho(s)$, yielding values that increase with energy (table 2) with positive curvature (figures 6 and 7). Experimentally, total cross-sections increase with energy as $\ln s$ or $\ln 2s$ in the concerned energy range, and soft processes are expected to have a $\ln s$ behaviour. From the optical theorem, the interdependence of the free parameters and the physical observable (equation (6)) may be connected with the unitary condition, for which lowest order cross-sections within the frame of gauge field theories have $\ln s$ terms [63]. The fits, extrapolations, and constraints led naturally to $\ln s$ terms appearing in the two-energy dependent parameters $C(s)$ and $\alpha^{-2}(s)$, and therefore the hypothesis of polynomial functions of $\ln s$ seems quite reasonable.

As for the parameter $\lambda(s)$ a basic property of the 'Glauber multiple diffraction model' is to associate elastic scattering cross-sections of nucleons with the scattering amplitude of their composite partons [51]. Within this framework, the ratio of the real and imaginary parts of the
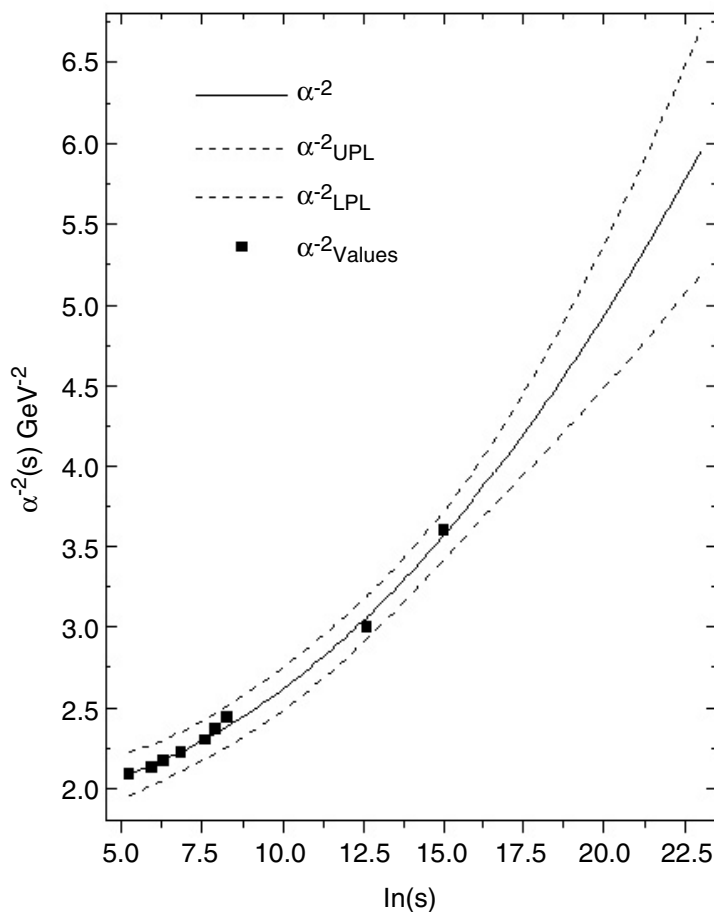
Figure 7. The parameter $\alpha^{-2}(s)$ from table 2 with its confidence interval.

parton–parton amplitudes (equation (12)), $\lambda(s) = \mathrm{Re}\ f(q, s)/\mathrm{Im}\ f(q, s)$ behaves on the partonic scale as $\rho(s)$ behaves on the hadronic scale. The influence of $\lambda(s)$ on the hadronic amplitude has been empirically analysed in [7], showing that if $\lambda(s)$ increases (or decreases), $\rho(s)$ also increases (or decreases) (figure 9), and $\lambda(s) = 0$ at the same energy value where $\rho(s) = 0$. However, due to the lack of $\rho(s)$ data above the experimental energy range used in this work, the parametrization of $\lambda(s)$ at high energies is based on the conventional assumption that beyond $\sqrt{s} \sim 100\,\mathrm{GeV}$, $\rho(s)$ has a maximum and then goes asymptotically to zero [37], the rate of convergence depending on the particularities of the model. Considering this and the empirical behaviour of $\lambda(s)$, shown in table 2, we propose the parametrization given in equation (19), where $s_0 = 400\,\mathrm{GeV}^2$ is the value at which $\lambda(s)$ converges to zero, and the numerical coefficients control the maximum and asymptotic behaviour.

Recall that blackening and expansion are very well-known properties of elastic scattering. Within the context of the present empirical analysis, blackening and expansion are related to the elementary parton–parton amplitude and the hadronic form factors through the energy-dependent parameters $C(s)$ and $\alpha(s)$ respectively. Since in the straight forward direction the scattering amplitude is basically of diffractive nature and the eikonal becomes purely imaginary, for hadron–hadron $\xi(b, s) = C(s)\langle G^2 \mathrm{Im}\ f(q, s)\rangle = \mathrm{Im}\ \Omega(b, s)$, so that in terms of equations (9) and (11) the opacity satisfies $\Omega(b, s) \geqslant 1$, and the free parameter $C(s)$ behaves as an absorption factor (optical theorem). On the other hand, the free parameter $\alpha(s)^2$ may be connected to the
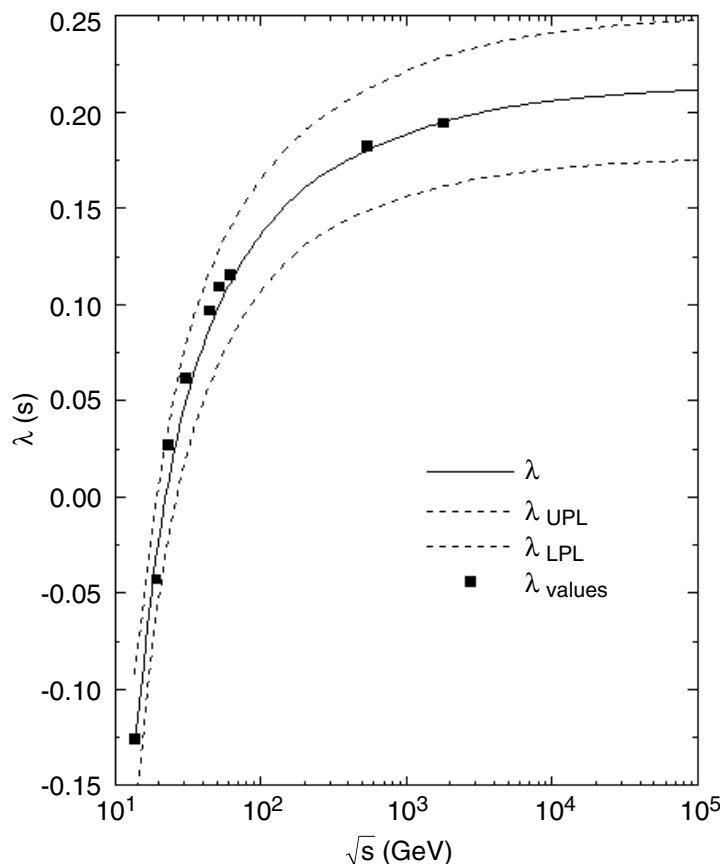
Figure 8. The parameter $\lambda(s)$ from table 2 with its confidence interval.

hadronic radius [7] as $R^2(s) = -6[dG(q, s)/dt]_{t=0}$. Then, from equation (9)

$$R^2(s) = 0.2332 \left[\frac{1}{\alpha^2(s)} + \frac{1}{\beta^2(s)} \right] (fm)^2.$$

Therefore, from equation (18) and the adopted value $\beta^2 = 1.8\,\text{GeV}^2$ the radius is an increasing function of energy and such a behaviour expresses the expansion effect. The result is that hadrons become blacker and larger as energy increases, consistent with the so-called 'Bell effect' [64]. Since the hadronic scattering amplitude is purely imaginary, the free parameters may be associated with the physical observable by means of equations (6) and (7).

6. The extrapolation procedure

The procedure followed to obtain predictions of σ_{tot}^{pp} at high energies with confidence intervals based on the 'forecasting' statistical method described in appendix is as follows.

(i) For each energy-dependent parameter, using the values displayed in table 2, we set up predictive equations of interpolative type equation (A.4) for use within the data range and of extrapolative type equation (A.6) for use out of range.
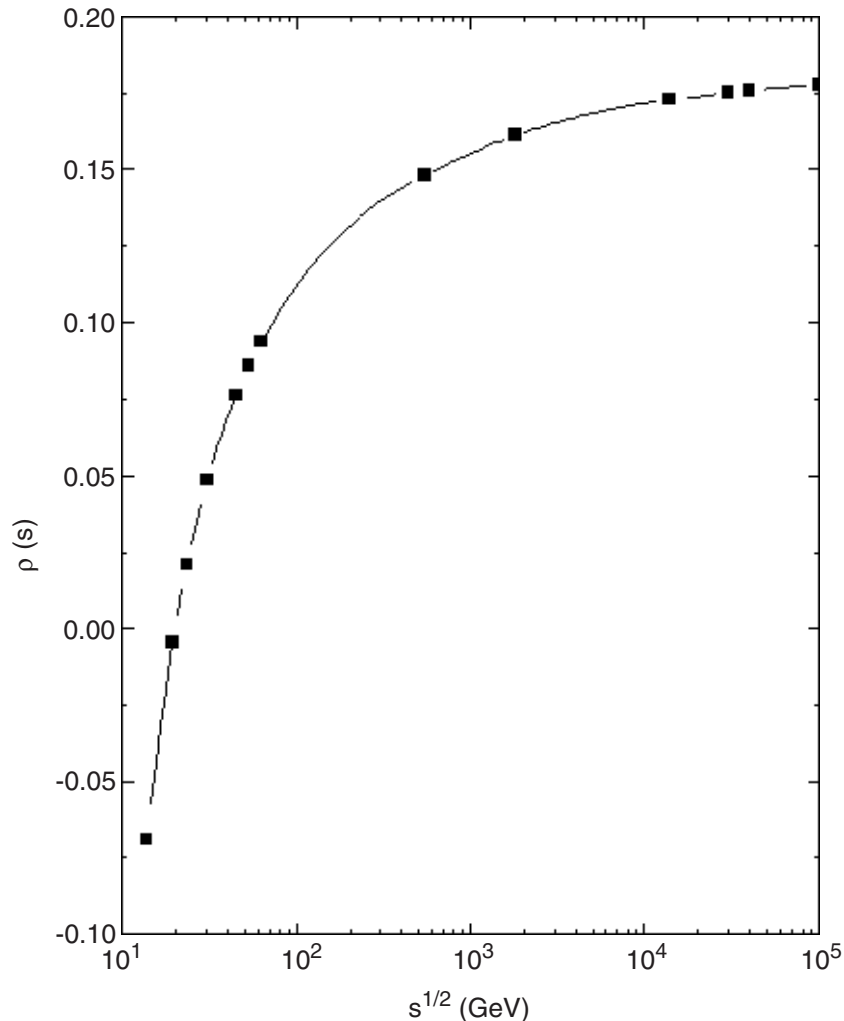
Figure 9. Data behaviour of the parameter $\rho(s)$ at $\sqrt{s} \leqslant 62.5$.

(ii) Using the least-squares method in matrix formalism, as described in the appendix (equations (A.10)–(A.12)) we obtained the constants $\hat{\beta}_0, \hat{\beta}_1, \hat{\beta}_2$ for each of the parameters. The autocorrelation constant was determined as described in [65, 66].

(iii) With the values above, the central values of the three parameters (equations (17)–(19)) were obtained, leading to a second-order fitting of the values of $C(s)$ and $\alpha^{-2}(s)$ and an exponential fit of $\lambda(s)$. Results are shown in table 3.

(iv) We evaluated the variance for each of the newly determined values (equation (A.14)).

(v) Using equations (A.15) and (A.16), we estimated the confidence intervals for each of the interpolated–extrapolated values, such that by fitting the extreme values of these confidence intervals, we built the error bands of each of the parameters, as is shown in figures 6–8.

(vi) The 'central values' of σ_{tot}^{pp} for each point are obtained by introducing in equations (15) and (16) the values of $C(s)$, $\alpha^{-2}(s)$ and $\lambda(s)$ (displayed in table 2).

Table 3. Fitted values (interpolation and extrapolation) of $C(s)$, $\alpha^{-2}(s)$ and $\lambda(s)$.

$\sqrt{s}$ (GeV)	$C(s)$ (GeV^{-2})	$\alpha^{-2}(s)$ (GeV^{-2})	$\lambda(s)$
13.8	9.9039	2.0945	-0.12816
19.4	10.082	2.1469	-0.02848
23.5	10.225	2.1798	0.00975
30.7	10.474	2.2296	0.04942
44.7	10.923	2.3075	0.08786
52.8	11.159	2.3451	0.10064
62.5	11.421	2.3849	0.11172
546	16.872	3.0634	0.18035
1800	21.518	3.5685	0.19501
14 000	32.239	4.6555	0.20703
16 000	33.056	4.7359	0.20749
30 000	37.102	5.1298	0.20927
40 000	39.062	5.3188	0.20993
100 000	45.757	5.9568	0.21153

(vii) Finally, the overall confidence band for the predicted σ_{tot}^{pp} is obtained, not from equations (A.15) and (A.16), but from the substitution of the extreme values of the error bands of the three energy-dependent parameters into equations (15) and (16), followed by the corresponding fits (figures 10 and 11).

7. Results

The total cross-sections with their respective errors are summarized in table 4. For $\sqrt{s} \leqslant$ 62.5 GeV data were taken from [59] and for 546 GeV, from [33]. For the value at 1800 GeV there exist three different measurements: the value of the 'CDF Collaboration' (80.3 ± 2.24 mb) [35], the value of the 'E710 Collaboration' (72.8 ± 3.1 mb) [34] and the value of the 'E811 Collaboration' (71.7 ± 2.02 mb) [36].

    There is controversy over whether the correct value is that of the 'CDF Collaboration' or of the lower values of the 'E710 Collaboration' and the 'E811 Collaboration', mainly related to the estimation of the different backgrounds. For instance, the 'CDF Collaboration' has decided to use only its σ_{tot}^{pp} value to quote luminosity values for all of its physics programmes [70] whereas the 'Tevatron Collaboration', D0, has adopted the average of the three measurements [70]. For this work, one of us (J V) suggested following this second option to use the arithmetic weighted mean of the three values (74.91 ± 1.35 mb). The effect on our results of the different values of the three collaborations is mentioned in the next section. We quote in table 4 the values of the predicted σ_{tot}^{pp} for two different energy intervals: σ_{tot}^{1800} ($13.8 \leqslant \sqrt{s} \leqslant 1800$ GeV), and σ_{tot}^{546} ($13.8 \leqslant \sqrt{s} \leqslant 546$ GeV). Figure 10 represents graphically the first case together with cosmic ray data. For further discussion, we include in table 4 predicted values from two standard accelerator-based data extrapolations: the first one, $\sigma_{546}^{[21]}$ makes a fit to all σ_{tot}^{pp} and $\sigma_{tot}^{\bar{p}p}$ data in the interval $10 \leqslant \sqrt{s} \leqslant 546$ GeV using expression (2) [21], and the second one, $\sigma_{\rho}^{[6]}$ (figure 1), in the same energy range, makes the simultaneous fit to all σ_{tot}^{pp}, $\sigma_{tot}^{\bar{p}p}$, ρ_{tot}^{pp} and $\rho_{tot}^{\bar{p}p}$ data through the method described in section 2 [6].

Table 4. Central, upper and lower values for σ_{tot} obtained with the procedure of section 6 and the method described in the appendix. The $\sigma_{tot}^{1800}, \sigma_{tot}^{546}, \sigma_{tot}^{62.5}$ columns include data up to 1800, 546, 62.5 GeV respectively. The quoted $\sigma_{546}^{[21]}$ and $\sigma_{\rho}^{[6]}$ values are from [21] and [6] respectively.

$\sqrt{s}$ (GeV)	σ_{tot}^{exp} (mb)	σ_{tot}^{1800} (mb)	$\sigma_{546}^{[21]}$ (mb)	σ_{tot}^{546} (mb)	$\sigma_{\rho}^{[6]}$ (mb)	$\sigma_{tot}^{62.5}$ (mb)
13.8	38.36 ± 0.04	$38.29^{+1.06}_{-0.98}$	–	$38.30^{+0.94}_{-0.92}$	–	$38.51^{+0.62}_{-0.56}$
19.4	38.97 ± 0.04	$38.92^{+0.98}_{-0.97}$	–	$38.82^{+0.88}_{-0.87}$	–	$38.82^{+0.59}_{-0.54}$
23.5	38.94 ± 0.17	$39.44^{+0.97}_{-0.96}$	–	$39.44^{+0.88}_{-0.86}$	–	$39.26^{+0.62}_{-0.58}$
30.7	40.14 ± 0.17	$40.34^{+0.99}_{-0.95}$	–	$40.37^{+0.88}_{-0.88}$	–	$40.15^{+0.66}_{-0.61}$
44.7	41.79 ± 0.16	$41.93^{+1.06}_{-0.96}$	–	$42.00^{+0.93}_{-0.92}$	–	$41.93^{+0.66}_{-0.62}$
52.8	42.67 ± 0.19	$42.76^{+1.09}_{-0.98}$	–	$42.84^{+0.95}_{-0.94}$	–	$42.93^{+0.69}_{-0.64}$
62.5	43.32 ± 0.23	$43.67^{+1.13}_{-0.99}$	–	$43.77^{+0.98}_{-0.97}$	–	$44.05^{+0.78}_{-0.72}$
546	61.5 ± 1.5	$61.62^{+1.58}_{-0.94}$	–	$61.78^{+1.33}_{-1.29}$	–	$69.39^{+8.4}_{-7.4}$
1800	74.91 ± 1.35^a	$76.17^{+2.02}_{-1.07}$	76.7 ± 4.0	$76.00^{+2.41}_{-2.34}$	76.5 ± 2.3	$91.74^{+16.9}_{-14.7}$
14 000	–	$108.27^{+4.72}_{-3.17}$	112 ± 13.0	$106.5^{+6.56}_{-6.55}$	–	$143.86^{+38.6}_{-33.5}$
16 000	–	$110.67^{+5.00}_{-3.40}$	–	$108.7^{+6.94}_{-6.94}$	111.0 ± 8.0	$147.85^{+40.3}_{-35.1}$
30 000	–	$122.41^{+6.40}_{-4.62}$	–	$119.6^{+8.83}_{-8.96}$	–	$167.64^{+48.9}_{-42.6}$
40 000	–	$128.05^{+7.08}_{-5.27}$	–	$124.7^{+9.83}_{-9.97}$	130.0 ± 13.0	$177.23^{+53.1}_{-46.3}$
100 000	–	$147.14^{+9.63}_{-7.68}$	–	$142.0^{+13.33}_{-13.7}$	–	$210.06^{+67.6}_{-59.1}$

^{a} This value is the weighted arithmetic mean of the E710 (72.8 ± 3.1 mb), CDF (80.3 ± 2.3 mb) and E811 (71.7 ± 2.0 mb) values.

8. Discussion

Let us first examine what happens when our main assumption, the asymptotic equality of σ_{tot}^{pp} and $\sigma_{tot}^{\bar{p}p}$, is not used. Analysis of figure 11 shows that if we limit our fitting calculations to the accelerator domain $\sqrt{s} \leqslant 62.5$ GeV, where σ_{tot}^{pp} data exist, the extrapolation at cosmic ray energies produces an error band so large that potentially any cosmic ray result becomes compatible with results at accelerator energies. It can be seen that, in this case, the σ_{tot}^{pp} values obtained when extrapolated to ultra high energies seem to confirm the highest quoted values of the cosmic ray experiments [9, 30]. Also it can be noted that such extrapolation to ultra high energies may claim not only agreement with the analysis carried out in [30] and the experimental data of the Fly's Eye [9], but even with the Akeno Collaboration [43], because their experimental errors are so big that they overlap with the errors reported in [9], and of course fall within the predicted error band for that case $\sqrt{s} \leqslant 62.5$ GeV (figure 11). If true, that would imply that the extrapolations cherished by experimentalists are meaningless. But the prediction shown in figure 11 gives $\sigma_{tot}^{pp} = 69$ mb at the CERN $S\bar{p}pS$ Collider (546 GeV), and 91.6 mb at the Fermilab Tevatron (1.8 TeV). Comparing with table 1 we see that the measured $\sigma_{tot}^{\bar{p}p}$ at 546 GeV is smaller than the predicted σ_{tot}^{pp} by nearly 8 mb, and that at 1.8 TeV by more than 15 mb, which no available model is able to explain [38]. However, when the initial hypothesis, $\sigma_{tot}^{\bar{p}p} = \sigma_{tot}^{pp}$ asymptotically is used, then the existing $\sigma_{tot}^{\bar{p}p}$ data at higher accelerator energies may safely be included. This permits enlargement of the lever arm for the extrapolation by a great amount, and both the predicted values and the error band change considerably. This can be clearly seen in figure 10, as well as in table 4, where we have added the available $\sigma_{tot}^{\bar{p}p}$ up to 0.546 TeV (the σ_{tot}^{546} column) and up to
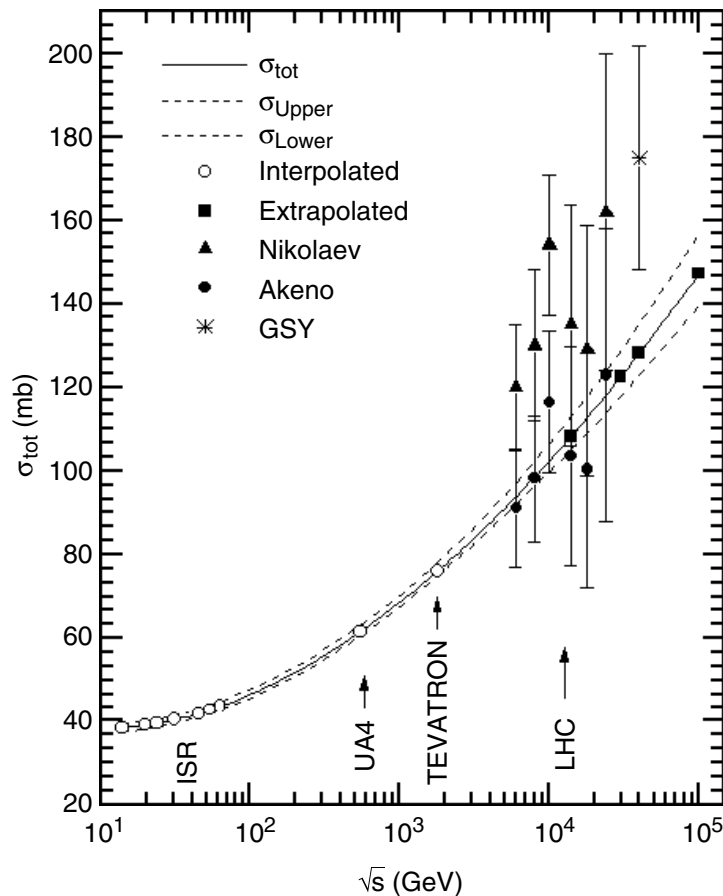
Institute *of* **Physics**   Φ DEUTSCHE PHYSIKALISCHE GESELLSCHAFT

Figure 10. Prediction of the total cross-section using data up to 1800 GeV (solid line), σ_{tot}^{1800}. The error band (dashed lines) is obtained as per section 6, that is, using the 'forecasting' method.

1.8 TeV (the σ_{tot}^{1800} column). Now the predicted value of σ_{tot}^{pp} from our extrapolation σ_{tot}^{1800}, for instance at $\sqrt{s} = 40$ TeV, $\sigma_{tot}^{pp} = 128.0_{-5.27}^{+7.08}$ mb, is seen to be incompatible with those in [9, 30] by several standard deviations, although not so different from the Fly's Eye or Akeno results, nor from the predicted value in [6].

The quoted error bands, obtained as described in section 6 and the appendix illustrate that the inclusion of 'residual correlations' in the 'forecasting' method produce a neat fit, irrespective of the parametrization model. This seems to be an advantage with respect to other statistical techniques. However, it must be emphasized that it is not valid to compare different statistical techniques when using different parametrization models, or when running the same parametrization with different input values. In spite of this, we would like to make a strict qualitative observation, in the sense that other parametrizations [6, 21] with similar input quantities (for instance ρ and $d\sigma/dt$) lead to central values that are only slightly higher than ours, whereas the quoted errors are larger than ours, some of them by nearly a factor of 3, as can be seen in table 4, or in figures 4 and 10. For instance, the quoted error in the fit σ_{tot}^{1800} at 100 TeV in the centre of mass (which corresponds to $\simeq 10^{19}$ eV in the laboratory), $147_{-7.68}^{+9.63}$, is comparable to (or even better than) the error obtained at much more lower energies in other works as can
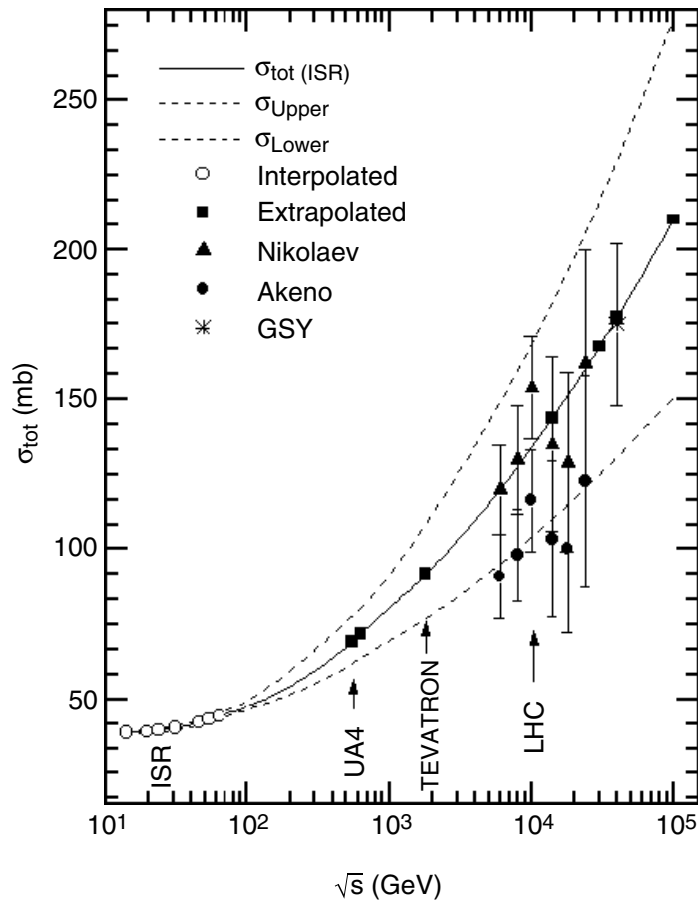
Figure 11. Prediction of the total cross-section using *pp* data up to 62.5 GeV (solid line). The error band (dashed lines) is obtained as described in section 6 and the appendix.

be seen in table 4, at 16 and 14 TeV ($\simeq 10^{17}$ eV in the laboratory), corresponding to the energy range of future LHC CERN Collider. Also, it can be appreciated from table 2 in [6], that the half width of the cross-section uncertainty bands, 7.2 and 10%, at 16 and 40 TeV respectively, is higher than the equivalent in this work, 6.4 and 7.9% (the values quoted in column 5 of table 4); in both cases the values of σ_{tot}^{pp} have been estimated using as lever arm the value at 546 GeV.

Obviously, these comments are only suggestive but important for the questions they raise: though it is clear from statistical theory that the forecasting technique is a highly precise method (section 6, appendix and references therein), its advantage over other techniques is, however, in principle only a second order effect (as inferred from equations (A.1) and (A.8)) when applied to the same conditions. Does the goodness-of-fit improve for certain parametrizations and input because the parametrization model is better? The answer must depend on a deep quantitative analysis, applying the forecasting method to different parametrization models of the total cross-section, in order to discern which model yields the best confidence estimates, with the goal of drawing more reliable physical inferences. Such an analysis is beyond the scope of the present paper and will be the subject of a forthcoming work.

9. Conclusions

It has been shown in this work that high CL extrapolations to high energy σ_{tot}^{pp} values are strongly dependent on the energy range covered and the available number of data values. In particular, if we limit the input σ_{tot}^{pp} accelerator data to the range $\sqrt{s} \leqslant 62.5\,\text{GeV}$, for the extrapolation to cosmic ray energies, the results are compatible with most of the cosmic ray experiments, and other predictive models [6], because the predicted error band is wide enough to cover their quoted errors (figure 11). However, as data to be extrapolated reach higher energies, including $\sigma_{tot}^{\bar{p}p}$ data up to 1.8 TeV, that is, when all experimental available data are taken into account, the curve is lowered by this last datum and the extrapolated error bands are much reduced. Accepting the accelerator extrapolations as indicative of the most probable σ_{tot}^{pp}, we conclude that they might help normalize the interpretation of cosmic ray experiments, perhaps, as an example, suggesting that the parameter k be kept free. The k value thus computed could help to tune the complicated Monte Carlo calculations used to evaluate the development of the showers induced by cosmic rays in the upper atmosphere. Extrapolations from our parametrization model would imply that σ_{p-air}^{inel} should be smaller than usually considered, which would have important consequences for the development of high energy cascades.

Although it is quite clear that results of this work are based on the assumption $\sigma_{tot}^{pp} = \sigma_{tot}^{\bar{p}p}$ at energies in the range $546 \leqslant \sqrt{s} \leqslant 1800\,\text{GeV}$, the problem of a fast or slow rise of the cross-section at high energies will be only solved by the forthcoming very high energy colliders. The new Relativistic Heavy Ion Collider (RHIC) which has become operational at Brookhaven, should produce a value of σ_{tot}^{pp} at $\sqrt{s} = 500\,\text{GeV}$ very soon, allowing a comparison with the measured value of $\sigma_{tot}^{\bar{p}p}$ at $\sqrt{s} = 546\,\text{GeV}$. Later on, the LHC should give us a σ_{tot}^{pp} value at $\sqrt{s} = 14\,\text{TeV}$. If it could be run at 2 TeV, a direct comparison between its σ_{tot}^{pp} value and the $\sigma_{tot}^{\bar{p}p}$ found at the Tevatron could be made. Additionally, experiments such as the HiRes [2] and the Auger Observatory [3] will bring new light to the extrapolation problem, i.e. whether the real values of σ_{tot} are described by parametrizations consistent with a fast rise with high energies, to be called the 'cosmic result' (e.g. [71]) or with a slower rise with energy, to be called the 'accelerators result', the result presented in this paper. Instead of looking for a new physics based on 'exotic' events to explain the fast rise in energy of σ_{tot}, what we need is highly reliable data at intermediate energies $(2 \leqslant \sqrt{s} \leqslant 15\,\text{TeV})$ to be used as confidence lever arms for extrapolations, to more accurate σ_{tot} at cosmic ray energies. In should be kept in mind that extrapolations from accelerator data must be included in interpreting cosmic ray phenomena and determining cross-sections. Although there are basic differences of this work and the COMPETE Collaboration [22]–[28] regarding the model employed and the techniques for extrapolation, the statistical method for calculation of the confidence intervals and the value of the Tevatron collider cross-section data used, nevertheless, it must be noted that the conclusions reached are very similar (e.g. [26]). Another parametrization with central value predictions not so different from ours, is that of the 'Ensemble A', discussed in [67, 68].

Finally, it is worth mentioning that this work reduces the width of the confidence band around 'multiple diffraction' model fits of accelerator data, strengthening suspicions that this extrapolation disagrees with cross-sections derived from cosmic ray showers. The reasons for the disagreement can be in the theory and method of analysis of the showers, in misunderstandings of the measurements at both ends, in the incompleteness of our understanding of p–p cross-sections, etc. The recognition and quantification of the discrepancy contributed here is a necessary step. As the reduction in uncertainty is largely due to the inclusion of higher energy accelerator data

and clarified by the increased statistical analysis presented here, we are hopeful that additional data from current experimental work will result by similar computations in a more detailed picture allowing us to distinguish between competing models.

Acknowledgments

Appendix A

A.1. Confidence intervals of the model prediction

The process by which a statistical method reproduces the behaviour of the given data of any physical quantity with high fidelity precision sets the pattern for the prediction of out of the range data. In the context of pp and p̄p hadronic total cross-sections at very high energies, a great deal of work has been done outside the energy range of accelerators: accelerator predictions are usually compared to cosmic ray data, producing a disagreement which has also been widely discussed in the literature. Such a comparison depends critically on a high confidence band of uncertainty for any parametrization model. The validity of any statistical method to predict a given physical quantity out of the data range values (extrapolation) depends on its precision in reproducing the data used in the range (interpolation). A fundamental task of any prediction method is to minimize the error band of the predicted set of values. In the specific case of σ_{tot}, what is sought is to obtain a prediction beyond the energy range of the employed data with the minimum of dispersion. In this context, popular techniques are derived from the statistical theory known as 'regression analysis' either by the 'multiple regression' approach or on the simplest version, a 'simple regression analysis', both based on the method of 'least squares'. Among the important indicators of any statistical method within the frame of the present work there is the CL and the 'confidence intervals' (e.g. [69]).

For a given phenomenon characterized by an independent variable (x) that generates a response variable (y) 'regression analysis' supplies a procedure to estimate the corresponding statistics: to fit a set of data of the phenomenon in between the known points (interpolation), to estimate ($\bar{y}$) the mean value of y, to predict an extrapolated value of y beyond the known points (extrapolation) for a given value of x, and to build a confidence interval around each of the 'estimated' or 'prognosticated' values (for instance [72, 73]). In its general form, the dependent variable y can be written as a function of k independent variables $x_1, x_2, \ldots, x_k$, where the variables x_j may represent powers of these variables, cross-products of the variables, or even a parametric dependence of other variables (see for instance [74]). Statistical techniques of 'regression analysis' are based on the minimization of the quadratic sum of data deviations with respect to the mathematical function or general model $y(x_1, x_2, \ldots, x_k)$ used for the prediction. For a given distribution of residuals $R_i = y_i - \bar{y}_i$ a full set of confidence indicators are generated, where typical error bands (belts) for extrapolations up to m steps beyond the last $n - esim$ experimental point is given as

$$\text{Error } B = \bar{y}_{n+m} \pm t_{\delta/2}^{k-p} S_d, \tag{A.1}$$

where S_d^2 is the variance, defined as the square of the standard deviation (usually called the standard error of estimate), $\bar{y}_{n+m}$ is the corresponding central prediction and $t_{\{\delta/2\}}^{\{k-p\}}$ denotes the probability density function (pdf) known as the Student's t-distribution for the k values of the independent variables with p degrees of freedom, and a confidence coefficient $\delta/2$. However, the previous generalization does not incorporate effects related to the position of the experimental values of y around the employed central value, that is the correlation among residuals that generates the regression model [74]. In other words, no interaction terms are assumed, implying that each of the independent variables affects the response y independently of the other independent variables and the error ϵ associated with any one y value is independent of the error associated with any other y value. Such an omission of the residuals' correlation leads to a notorious modification of the statistical estimators.

A.2. *The forecasting method*

The above limitation, can be surmounted by identifying the obtained dataset $(x_{1i}, x_{2i}, x_{3i}, \ldots, x_{ki}; y_i)$ with a time series, and then evaluating the correlation among consecutive residuals (the so-called autocorrelation procedure, of which the simplest one is the autoregressive 1st-order model). The forecasting statistical method is based on autocorrelation models adopted for the evaluation of the correlation among consecutive residuals, in and out of the data set by means of an iterative process [74]. In general, this procedure modifies the fitting constants of the model and the estimated variance of residuals and minimizes the width of the error intervals for interpolation or (extrapolation), in the process increasing the CL of predictions [74]. To quantify the effect that the autocorrelation of residuals has on the regression model and associated estimators, let us represent such a model by a response variable $y = E(y) + \epsilon$, where

$$E(y) = \beta_0 + \beta_1 x_1 + \beta_2 x_2 + \cdots + \beta_k x_k, \tag{A.2}$$

represents the deterministic component of the proposed regression model; $x_1, x_2, \ldots, x_k$ are the independent variables, accepted as assigned and may represent higher order terms and even functions of variables as long as the functions do not contain unknown parameters; $\beta_1, \beta_2, \ldots, \beta_k$ are the unknown coefficients to be determined by the least-squares method, representing the contribution of the independent variables x_i, and ϵ represents the random error component. For the evaluation of residuals $R_i = y_i - E(y_i)$ it is assumed they have a normal distribution with mean zero and constant variance. In the autoregression model of first order each residual R_i is related with the previous one as

$$R_i = \phi R_{i-1} + r_i, \tag{A.3}$$

where ϕ is the autocorrelation constant among the residuals ($|\phi| < 1$) [65, 66], and r_i in this case is a residual called white noise, uncorrelated with any other residual component. The incorporation of the effect of autocorrelation of residuals to the solution of the regression problem through equation (A.2) leads to a modification of the regression constants and the corresponding variance: using the data set, the estimate of the $k + 1$ regression constants of equation (A.2) and the constant ϕ is obtained from the autocorrelation model according to the following interpolation equation for the response variable $\hat{y}_i$:

$$\hat{y}_i = \hat{\beta}_0 + \hat{\beta}_1 x_{1,i} + \hat{\beta}_2 x_{2,i} + \cdots + \hat{\beta}_k x_{k,i} + \hat{\phi} \hat{R}_{i-1}, \tag{A.4}$$

where $i = 1, \ldots, n$, $x_{k,i}$ represents the independent variable x_k corresponding to the point (i), the small hat indicates estimated values, and the mean of the residual white noise has been taken as $\bar{r}_{n+1} = 0$. The prediction of values beyond the nth data value, beginning for instance with y_{n+1}, is then given as

$$y_{n+1} = \hat{\beta}_0 + \hat{\beta}_1 x_{1,n+1} + \hat{\beta}_2 x_{2,n+1} + \cdots + \hat{\beta}_k x_{k,n+1} + R_{n+1}, \tag{A.5}$$

where $x_{k,n+1}$ represents the independent variable x_k corresponding to the point $(n + 1)$. The forecasted response variable $\hat{y}_{n+1}$ is

$$\hat{y}_{n+1} = \hat{\beta}_0 + \hat{\beta}_1 x_{1,n+1} + \hat{\beta}_2 x_{2,n+1} + \cdots + \hat{\beta}_k x_{k,n+1} + \hat{\phi} \hat{R}_n. \tag{A.6}$$

Similarly, for the next value $\hat{y}_{n+2}$,

$$\hat{y}_{n+2} = \hat{\beta}_0 + \hat{\beta}_1 x_{1,n+2} + \hat{\beta}_2 x_{2,n+2} + \cdots + \hat{\beta}_k x_{k,n+2} + (\hat{\phi})^2 \hat{R}_n \tag{A.7}$$

and so on successively. That is, the estimation of extrapolated values is an iterative process where every new estimate makes use of the previous residual. Unfortunately, as we move farther from the last datum, the potential error increases due to possible changes in the structure of the regression model, or to changes in the variance value as the procedure continues. The problem can be surmounted by estimating the variance associated with each prognostic (estimated variance) through the correlation constant ϕ. Thereby, according to the autoregressive model of first-order within the data range up to the data n, we have a constant variance S_f^2, and for one step out of the data range (i.e. $n + 1$) the corresponding variance is $S_{f,n+1}^2 = S_f^2[1 + \phi^2]$, whereas for two steps beyond $(n + 2)$ the estimated variance is $S_{f,n+2}^2 = S_f^2[1 + \phi^2 + \phi^4]$; and for m steps beyond the range $(n + m)$ the estimated variance is $S_{f,n+m}^2 = S_f^2[1 + \phi^2 + \phi^4 + \cdots + \phi^{2(m-1)}]$. On this basis, for a prediction interval with a confidence of $100(1 - \delta)\%$ and a type t–Student distribution, the amplitude of the regression intervals for $(n + m)$ steps beyond the nth data value is given in [74], as

$$Error B = \hat{y}_{n+m} \pm t_{\delta/2}^{k-p} \sqrt{S_f^2[1 + \phi^2 + \phi^4 + \cdots + \phi^{2(m-1)}]}. \tag{A.8}$$

Due to the incorporation of the autocorrelation of residuals, the error bands evaluated in this way give a higher CL than other methods of regression analysis which ignore this effect [74]. This translates into a decrease in the width of the prediction intervals following the decrease of the estimated variance (e.g. table 9.7 in [74]). It must be emphasized that technically the meaning of the error bars in different methods derived from regression analysis remains exactly the same, since they quantify the level of CL, that is, they express the probability that the 'true answer' will fall with $100(1 - \delta)\%$ of probability within the bands, when other measurements are made under the same conditions. However, even if the concept is the same, every method predicts a different value of CL: in the particular case of the forecasting regression method, the essential point is that it uses the additional factor of the autocorrelation among residuals, to improve (1) the central estimate value and (2) the width of the confidence intervals (error bars), where narrowing expresses higher CL [74].

A.3. Matrix approach in regression analysis

This fit method is based on multiple regression theory and consists in creating a prediction equation for a quantity y (dependent variable), which depends on k independent variables (x_i), that is

$$E(y) = \sum_{i=0}^{k} \beta_i f_i(x_i), \tag{A.9}$$

with $f_o(x_o) = 1$, where f_i are arbitrary functions of x_i, and β_i are the regression constants. In the generalized version, the variable x_i may depend on other parameters, i.e., $x_i = x_i(s, t, \ldots)$. Therefore, the application of a multiple regression model to a given problem leads to a system of n equations with n incognitos, so that its solution is better obtained through a matrix formalism. Denoting by Y the matrix of ($n \times 1$)-dimension of the dependent variables and by X the matrix of $[n \times (k+1)]$-dimensions of the k independent variables, the row 1, $x_{11}, x_{12}, \ldots, x_{1k}$ multiplied by the column matrix of the βs determines the value y_1 of the dependent variable, the row 1, $x_{21}, x_{22}, \ldots, x_{2k}$ multiplied by the column matrix of the βs determines the value y_2 and so on:

$$X = \begin{pmatrix} 1 & x_{11} & x_{12} & \cdots & x_{1k} \\ 1 & x_{21} & x_{22} & \cdots & x_{2k} \\ \vdots & \vdots & \vdots & \ddots & \vdots \\ 1 & x_{n1} & x_{n2} & \cdots & x_{nk} \end{pmatrix}; \qquad Y = \begin{pmatrix} y_1 \\ y_2 \\ \vdots \\ y_n \end{pmatrix}; \qquad \mathcal{B} = \begin{pmatrix} \beta_0 \\ \beta_1 \\ \vdots \\ \beta_k \end{pmatrix}.$$

The variables contained in the matrixes X, Y can be related by the matrix equation $Y = X\mathcal{B}$, which is the matrix expression of the prediction equation (A.9). The $[(k+1) \times 1]$-dimensional matrix $\mathcal{B}$ contains the values of the constants β_i needed to write in explicit form the prediction equation (A.9). The βs can be determined by the least-squares method [74] through the condition

$$\sum_{j=1}^{n} [y_j - E(y_j)]^2 = \sum_{j=1}^{n} R_j^2 = \text{minimum}, \tag{A.10}$$

where y_j is the jth measurement of the response variable and $E(y_j)$ is the estimated central value with equation (A.9). The condition (A.10) is satisfied when $\frac{\partial}{\partial \beta_i} \sum_{j=1}^{n} R_j^2 = 0$, $(i = 1, \ldots, k)$, leading to a system of n equations with $k(= n)$ unknowns. This system in matrix form can be written (e.g. [75]) as

$$(X^t X)\hat{\mathcal{B}} = X^t Y, \tag{A.11}$$

where X^t denotes the transposed matrix of X and $\hat{\mathcal{B}}$ is the matrix of the expected values of the βs. From (A.11) we obtain the solution of equation (A.10):

$$\hat{\mathcal{B}} = (X^t X)^{-1} X^t Y, \tag{A.12}$$

where $(X^t X)^{-1}$ denotes the inverse matrix of $X^t X$. Essentially, this equation minimizes the quadratic sum of the deviations of points y_j with respect to the fitted function (A.9) ([74] p 783). With the previous matrices, several statistical estimators are easily determined, such as the sum

of square errors (SSE)

$$SSE = Y^t Y - \hat{\mathcal{B}}^t (X^t Y) \tag{A.13}$$

and the variance required to evaluate the confidence intervals, which is

$$S_f^2 = \frac{SSE}{[n - (k+1)]}, \tag{A.14}$$

where the denominator defines the number of degrees of freedom for errors, given by the number of β_i-parameters. Once the 'central' values are known, we evaluate the confidence interval for a particular value of the response variable, y_p, using the matrix of the particular values of the independent variables which determine the estimated value of y_p. Such a matrix, namely $\mathcal{A}$, denotes the column-matrix of $(k+1) \times 1$ dimensions, where elements $\{1, x_{1p}, x_{2p}, \ldots, x_{kp}\}$ correspond to the numerical values of the β_i appearing in equation (A.9). Therefore, the confidence interval for prediction within the range of data is determined as ([74], p 795):

$$\text{Interp } B = \hat{y} \pm t_{\delta/2}^{n-p} \sqrt{S_f^2 A^t (X^t X)^{-1} A} \tag{A.15}$$

and for extrapolation as ([74], p 800):

$$\text{Extrap } B = \hat{y} \pm t_{\delta/2}^{n-p} \sqrt{S_f^2 [1 + A^t (X^t X)^{-1} A]}. \tag{A.16}$$

Here $\hat{y}$ denotes the central prediction, A^t is the transposed matrix of A. Interp $B(+)$, Extrap $B(+)$ and Interp $B(-)$, Extrap $B(-)$ denote the corresponding upper and lower bounds respectively. $t_{\{\delta/2\}}^{\{n-p\}}$ denotes Student's t-distribution for the n values of the independent variables with p degrees of freedom. Estimates have been made with a precision of $100(1 - \delta)\%$, assuming $\delta/2 = 0.025$, which corresponds to a value of 95%.

References

[1] Engel R, Gaisser T K, Lipari P and Stanev T 1998 *Phys. Rev.* D **58** 014019
[2] See http://sunshine.chpc.utah.edu/research/cosmic/hires/
[3] February 1997 *The Pierre Auger Project Design Report (Fermilab report)*
[4] Lipari P 2003 *Los Alamos National Laboratory e-print* hep-ph/0301196 v1
[5] Donnachie A and Landshoff P V 1992 *Phys. Lett.* B **296** 227
[6] Augier C *et al* 1993 *Phys. Lett.* B **315** 503
[7] Martini A F and Menon M J 1997 *Phys. Rev.* D **56** 4338
[8] Block M M and Cahn R N 1985 *Rev. Mod. Phys.* **57** 563
[9] Gaisser T K, Sukhatme U P and Yodh G B 1987 *Phys. Rev.* D **36** 1350
[10] Dias de Deus J and Kroll P 1978 *Acta Phys. Pol.* B **9** 159
[11] Gaulianos K 1983 *Phys. Rep.* **101** 169
[12] Chou T and Yang C N 1967 *Proc. 2nd Int. Conf. on High Energy Physics and Nuclear Structure (Rehovot, Israel)* ed G Alexander (Amsterdam: North-Holland)
[13] Gribov V N 1969 *Zh. Eksp. Teo. Fiz.* **56** 892 [*Sov. Phys.—JETP* **29** 483]
[14] Kang K and Kim S K 1995 *Preprint* hep-ph/9510438
[15] Amaldi U *et al* 1977 *Phys. Lett.* B **66** 390

[16] Donnachie A and Landshoff P V 1979 *Z. Phys.* C **2** 55
[17] Amaldi U and Schubert K R 1980 *Nucl. Phys.* B **166** 301
[18] Donnachie A and Landshoff P V 1983 *Nucl. Phys.* B **231** 189
[19] Donnachie A and Landshoff P V 1984 *Nucl. Phys.* B **244** 322
[20] Donnachie A and Landshoff P V 1986 *Nucl. Phys.* B **267** 690
[21] Bueno A and Velasco J 1996 *Phys. Lett.* B **380** 184
[22] Nicolescu B, Cudell J R, Ezhela V V, Gauron P, Kang K, Kuyanonv Yu V, Lugovsky S B and Tkachenko N P (COMPETE Collaboration) 2001 *Preprint* hep-ph/0110170
[23] Nicolescu B, Cudell J R, Ezhela V V, Gauron P, Kang K, Kuyanonv Yu V, Lugovsky S B, Razuvaev E A and Tkachenko N P (COMPETE Collaboration) 2002 *Preprint* hep-ph/0209206
[24] Cudell J R, Ezhela V V, Gauron P, Kang K, Kuyanonv Yu V, Lugovsky S B, Martynov E, Nicolescu B, Razuvaev E A and Tkachenko N P (COMPETE Collaboration) 2002 *Preprint* hep-ph/0212101
[25] Cudell J R, Ezhela V V, Gauron P, Kang K, Kuyanonv Yu V, Lugovsky S B, Nicolescu B and Tkachenko N P (COMPETE Collaboration) 2002 *Phys. Rev.* D **65** 074024
[26] Cudell J R, Ezhela V V, Gauron P, Kang K, Kuyanonv Yu V, Lugovsky S B, Martynov E, Nicolescu B, Razuvaev E A and Tkachenko N P (COMPETE Collaboration) 2002 *Phys. Rev. Lett.* **89** 201801
[27] Cudell J R, Kang K and Kim S K 1997 *Phys. Lett.* B **395** 311
[28] Cudell J R, Ezhela V V, Kang K, Lugovsky S B and Tkachenko N P 2000 *Phys. Rev.* D **61** 034019
[29] Glauber R J and Matthiae G 1970 *Nucl. Phys.* B **21** 135
[30] Nikolaev N N 1993 *Phys. Rev.* D **48** R1904
[31] Amaldi U *et al* 1973 *Phys. Lett.* B **44** 11
[32] Amendolia S R *et al* 1973 *Phys. Lett.* B **44** 119
[33] Bozzo M *et al* 1984 *Phys. Lett.* B **147** 392
[34] Amos N A, Avila C, Baker W F, Bertani M, Block M M and Dimitroyannis D A 1989 *Phys. Rev. Lett.* **63** 2784
[35] Abe *et al* 1994 *Phys. Rev.* D **50** 5550
[36] Avila C *et al* 1999 *Phys. Lett.* B **445** 419
[37] Matthiae G 1994 *Rep. Prog. Phys.* **57** 743
[38] *Proc. Int. Conf. and 8th Blois Workshop on Elastic and Diffractive Scattering (EDS 99)*, (Protvino, 27 June–2 July 1999)
[39] Froissart M 1961 *Phys. Rev.* **123** 1053
     Martin A 1966 *Nuovo Cimento* **42** 930
[40] Augier C *et al* 1993 *Phys. Lett.* B **316** 448
[41] Lukaszuk L and Nicolescu B 1973 *Nuovo Cimento Lett.* **8** 405
[42] Gauron P, Lipatov L and Nicolescu B 1993 *Phys. Lett.* B **304** 334
[43] Honda M, Nagano M, Tonwar S, Kasahara K, Hara T, Hayashida N, Matsubara Y, Teshima M and Yoshida S 1993 *Phys. Rev. Lett.* **70** 525
[44] Baltrusatis R M, Cassiday G L, Elbert J W, Gerhardy P R, Ko S, Loh E C, Mizumoto Y, Sokolsky P and Steck D 1984 *Phys. Rev. Lett.* **52** 1380
[45] Baltrusatis R M *et al* 1985 *Proc. 19th ICRC, La Jolla*, vol 7, p 155
[46] Luna E G S and Menon M J 2001 On the total cross section extrapolations to cosmic-ray energies *Los Alamos National Laboratory e-print* hep-ph/0105076 v1
[47] Pryke C L 2000 *A comparative study of the depth of maximum of simulated air shower longitudinal profile*, *Preprint* astro-ph/0003442
[48] Hillas A M 1997 *Nucl. Phys. B (Proc. Suppl.)* **52** 29
[49] Fletcher R S *et al* 1994 *Phys. Rev.* D **50** 5710
[50] Glauber R J 1956 *Lectures in Theoretical Physics* (Reading, MA: Interscience)
[51] Glauber R J and Velasco J 1984 *Phys. Lett.* B **147** 380
[52] Velasco J, Perez-Peraza J, Gallegos-Cruz A, Alvarez-Madrigal M, Faus-Golfe A and Sanchez-Hertz A 1999 *Proc. 26th ICRC, Utah* **1** 198

[53] Perez-Peraza J, Gallegos-Cruz A, Velasco J, Sanchez-Hertz A, Faus-Golfe A and Alvarez-Madrigal M 2000 *Int. Workshop on Observing Ultra High Energy Cosmic Rays from Space and Earth, Proc. AIP No. 566* 343

[54] Bourrely C, Soffer J and Wu T T 1984 *Nucl. Phys.* B **247** 15
Bourrely C, Soffer J and Wu T T 1985 *Phys. Rev. Lett.* **54** 757

[55] Carboni G *et al* 1985 *Nucl. Phys.* B **254** 697

[56] Cudell J R, Ezhela V, Kang K, Lugovsky S and Tkachenko N 1999 *Los Alamos National Laboratory e-print* hep-ph/9908218 v

[57] Menon M J 1996 *Can. J. Phys.* **74** 594

[58] Rubinstein R *et al* 1984 *Phys. Rev.* D **30** 1413

[59] Schubert K R 1979 *Tables on Nucleon–Nucleon Scattering, of the Landollt-Börnstein New Series of Numerical Data and Functional Relationships in Science and Technology* Vol I/9a, ed K H Hellwege (Berlin: Springer)

[60] Bozzo M *et al* (UA4 Collaboration) 1984 *Phys. Lett.* B **147** 385

[61] Bozzo M *et al* (UA4 Collaboration) 1984 *Phys. Lett.* B **155** 197

[62] Amos N *et al* (E710 Collaboration) 1990 *Phys. Lett.* B **247** 127

[63] Cheng H and Wu T T 1987 *Expanding Protons: Scattering at High Energies* (Cambridge, MA: MIT Press)

[64] Henzi R and Valin P 1983 *Phys. Lett.* B **132** 443
Henzi R and Valin P 1985 *Phys. Lett.* B **160** 167

[65] Fuller W A 1976 *Introduction to Statistical Time Series* (New York: Wiley)

[66] Chatfield Ch 1996 *The Analysis of Time Series* (London: Chapman and Hall)

[67] Avila R F, Luna E G S and Menon M J 2001 *Los Alamos National Laboratory e-print* hep-ph/0105065 v1

[68] Caravalho P A S, Martini A F and Menon M J 2003 *Los Alamos National Laboratory e-print* hep-ph/0312243 v1

[69] Montanet L *et al* 1994 *Phys. Rev.* D **50** 1271

[70] Albrow M *et al* 1999 Comparison of the Total Cross Sections Measurements of CDF and E811 *Fermilab-TM-2071*

[71] Yodh G B, Pal Y and Trefil J S 1972 *Phys. Rev. Lett.* **28** 1005

[72] Cramer H 1958 *Mathematical Method of Statistics* (Princeton, NJ: Princeton University Press)

[73] Eadie W T, Drijard D, James D, James F E, Ross M and Sadoulet B 1971 *Statistical Methods in Experimental Physics* (Amsterdam: North-Holland)

[74] Mendenhall W and Sincich T 1993 *A Second Course in Statistics: Regression Analysis* (Englewood Cliffs, NJ: Prentice-Hall)

[75] Basilevsky A *et al* 1983 *Applied Matrix Algebra in Statistical Sciences* (New York: North-Holland)